偏振遥感的中性点大气纠正方法研究

吴太夏，张立福，岑奕，黄长平，赵恒谦，孙雪剑

中国科学院 遥感与数字地球研究所，北京 100101

摘 要: 地表物体具有较强的偏振特性，因此可以作为偏振遥感的信息源。但是，大气的偏振效应强于地表的偏振效应，导致星载遥感器无法有效接收地表目标的偏振信息，大气的起振与退偏效应成为偏振遥感对地表目标进行观测和应用的一个瓶颈问题。本文提出一种利用大气中性点对偏振遥感中地表偏振效应与大气偏振效应进行分离的方法，通过天空中大气线偏振度为零的中性点区域进行对地观测，目的是去除大气偏振作用，进而最大限度地获取地表目标偏振信息。地面实验的结果验证了利用大气中性点进行大气纠正具有理论上的可行性。

关键词: 偏振遥感，大气中性点，大气纠正

中图分类号: TP721.1　　文献标志码: A

引用格式: 吴太夏，张立福，岑奕，黄长平，赵恒谦，孙雪剑. 2013. 偏振遥感的中性点大气纠正方法研究. 遥感学报，17(2): 235－247

Wu T X, Zhang L F, Cen Y, Huang C P, Zhao H Q and Sun X J. 2013. Neutral point consideration for a tmospheric correction in polarization remote sensing. Journal of Remote Sensing, 17(2): 235－247

1 引 言

在偏振遥感对地探测中，特别是在可见-近红外波段，大气散射光具有很强的偏振性，因此目前国际上实用的星载偏振传感器主要都是进行大气探测，研究大气光学厚度、气溶胶粒径大小等物理性质和大气光学性质等(Fan 等，2008; Cairns 等，2009)。由于地表物体也具有比较强的偏振性质，如水体、植被、建筑物等，这种偏振性质可以用作遥感探测(Breon 等，1995; Wu 和 Zhao，2005)，法国的 POLDER 传感器在设计时曾试图对地表目标进行多角度偏振观测，但在使用过程中发现大气的偏振作用过于强烈，地物的偏振反射信息常被它所淹没(Bicheron 等，1997; Nadal 和 Bréon，1999)。大气的偏振效应因而成为偏振遥感对地观测的一个瓶颈问题。如何将偏振遥感图像中地物的偏振反射信息与大气的偏振效应有效分离成为一个研究难题，目前还没有较好的解决方案。

大气中性点是天空中大气偏振度为零的点(或区域)。19 世纪初人们相继观测到天空中 3 个著名的大气中性点: Arago 中性点(1809 年)、Babinet 中性点(1840 年)和 Brewster 中性点(1842 年)(Miyazaki 等，2009)。其后，很多大气光学界的学者对其性质进行了相关研究。本文拟通过在大气中性点位置放置传感器进行对地观测，由于该点的线偏振度值为零，就能从遥感影像上最大限度地去除掉大气偏振作用，从而直接获取地表目标的偏振信息，达到地-气偏振效应分离的目的。本研究可为偏振遥感拓展到更广泛的研究空间提供参考并推动偏振遥感对地表目标观测研究的开展。

2 大气偏振分布和大气中性点

太阳辐射透过大气层到达地球表面，经过大气的散射，太阳辐射具有一定的偏振性，如果大气散射多为一次散射时，这种太阳辐射的偏振现象在天空中形成了一个有规律的偏振分布，又称为天空偏振模式图。

正常晴空天气条件下，在太阳垂直面上，天空中会出现 Arago 中性点，Babinet 中性点和 Brewster 中性点(图 1)。Arago 点位于反太阳点上方 20°—

收稿日期: 2012-05-15; 修订日期: 2012-08-15

基金项目: 国家自然科学基金(编号: 41101328, 61178065); 中国科学院知识创新工程青年人才领域前沿项目

第一作者简介: 吴太夏(1979—)，男，博士，助理研究员。主要研究高光谱遥感理论与应用。E-mail: wutx@irsa.ac.cn

通信作者简介: 张立福(1967—)，男，博士，研究员。主要研究高光谱遥感。E-mail: zhanglf@irsa.ac.cn

30°的位置; Babinet 点位于太阳上方约 15°—20°的位置,Brewster 点则位于太阳下 15°—20°的位置,两者皆与太阳在同一方向,且两者的位置随太阳高度角的变化而变化,当太阳高度角比较大时,Babinet 点和 Brewster 点之间比较接近; 当太阳达到天顶时,它们差不多就合并为一个点(盛裴轩 等,2003; M uheim等,2006)。太阳一侧的中性点与反日点一侧的中性点两两具有对称性,因此在理论上,在反日点的下方也会出现第 4 个中性点,即反 Babinet 中性点(anti-Babinet point),2002 年,通过探空气球观测确实发现了该点(Horvath 等,2002)。

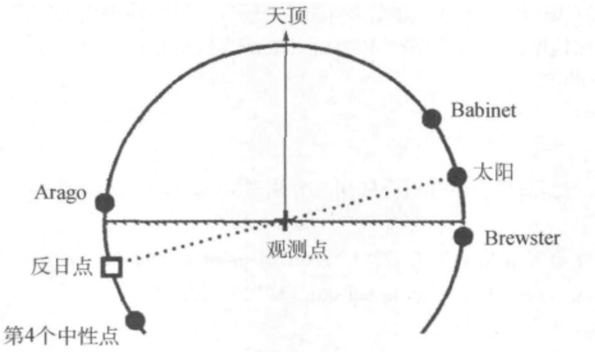

图 1 天空中的偏振中性点示意图

单次散射条件下,天空光的偏振一般为正值,但在多次散射条件下,大气粒子会造成负偏振。正负偏振交叉处的天空偏振度为零,即产生大气中性点(Coulson,1988; Horváth 和 Varjú,2004)。大气中性点一般处于太阳与天顶所在的主平面上,多次散射越强烈,大气中就会有越多的负偏振,同时中性点位置就会离理想状态下的位置越远。

大气中性点在天空中的位置与太阳高度息息相关。图 2 是 Chandrasekhar 利用理论模型计算得到的大气光学厚度为 0.10 时大气中性点的角度位置与太阳入射角在主平面上的关系曲线(Chandrasekhar 和 Elbert,1954)。

Babinet 中性点与太阳的位置密切相关,伴随着太阳升起到落下的全过程; 对于 Brewster 中性点,当太阳高度角约为 20°时开始出现,其位置与太阳的位置近乎线性相关,表现一致; 对于 Arago 中性点,只有当太阳高度角小于 20°时才会在天空中出现,即仅在早晚才能观测到。在其他大气光学厚度(0.15 或 0.20)时,中性点也具有相同的性质。

3 基于大气中性点的大气纠正方法

利用大气中性点进行大气纠正的主要思路是:

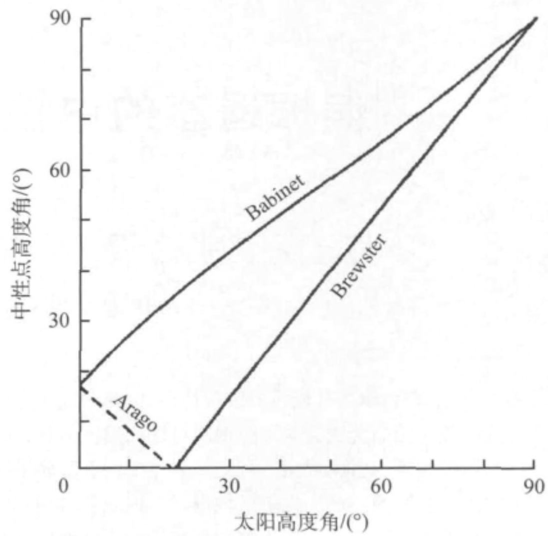

图 2 大气中性点位置与太阳高度角的关系图

将传感器对地表的观测方向与大气中性点区域的方向设置为一致,这时传感器到地表之间的大气偏振作用为零或减小到一定程度,达到大气偏振效应有效去除、地物偏振信息最大限度获取的目的。图 3是利用大气中性点进行大气纠正的示意图。图中大圆是地球大气的最外圈,离开大气散射,大气就没有偏振性,也就不存在中性点了,大圆的方向也是当天太阳升起和降落的轨迹。图中太阳的位置是虚拟的,表示太阳所在的方向。理论上,在地表与中性点连线方向上,传感器到地表的任何高度都可以观测到中性点,即机载和星载的传感器都有可能观测到中性点。

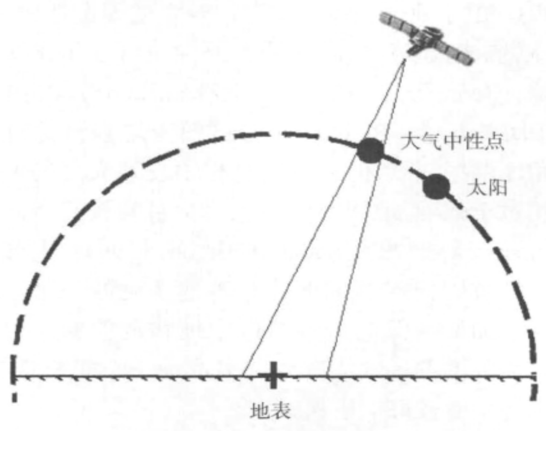

图 3 利用大气中性点对地偏振遥感的示意图

而在实际大气中,由于存在多次散射,中性点可能不是一个独立的点,而是天空偏振度为零(或接近于零)的一个区域; 另外,中性点也不是天空中固定的一个区域,而是以空中观测点为起点,方向

对着中性点区域的一个圆锥形的区域，在这个圆锥形区域里任何高度观测，其大气偏振度都近似为零。

3.1 天基观测的大气中性点性质

上述所讨论的大气中性点性质都是基于地基观测的结果，但遥感是一个自上而下的过程，与地基观测的方式相反，利用偏振中性点进行对地偏振遥感，最基本的问题是从天基能否观测到大气中性点。

图4是 Horváth 等人(2002)利用偏振相机在地面以及在3500 m 高空探空气球上拍摄的大气中性点，图中以黑色表示。拍摄时的当地太阳高度角均近似为0，图像上端的黑点为太阳，拍摄波长为红波段。图4(a)为地面拍摄结果，图4(b)为气球上拍摄结果。图4(b)说明了大气中性点可以在天基观测到。

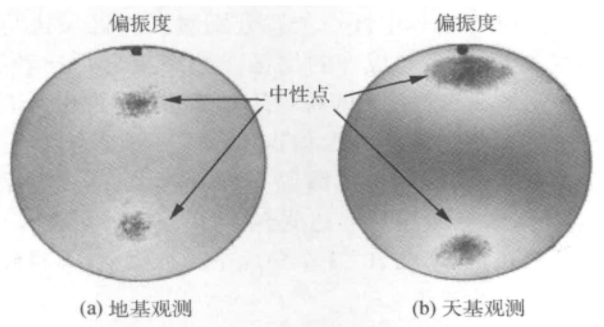

图4 地基与天基观测的大气中性点

图5是 Coulson(1959)给出的大气上行辐射与下行辐射的偏振中性点位置曲线图。图中显示的是中性点到反日点的角度距离与太阳高度角的函数曲线。大气光学厚度为1.0，实线和虚线分别是上行辐射和下行辐射曲线。上行辐射是由于大气粒子的后向散射造成的，它们与太阳(或反日点)的位置关系与下行辐射中的位置关系存在变化，所以上行辐射和下行辐射中的中性点名称是不一样的。地基观测到的3个常见中性点分别是 Arago 中性点、Babinet 中性点和 Brewster 中性点，天基观测到的3个中性点分别是：Brewster 中性点、反 Babinet 中性点和 Arago 中性点。图5中曲线 a 的实线和虚线分别是反日点下方的点和太阳下方的点的曲线，根据图1，分别为 Arago 点和 Brewster 点的曲线；曲线 b 的实线和虚线分别为反 Babinet 点和 Babinet 点的曲线。

从图5可以看出，对于曲线 a，当太阳高度角为60°—90°时，上行辐射的中性点(Arago 点)与下行辐射中性点(Brewster 点)的位置完全一致，当太阳

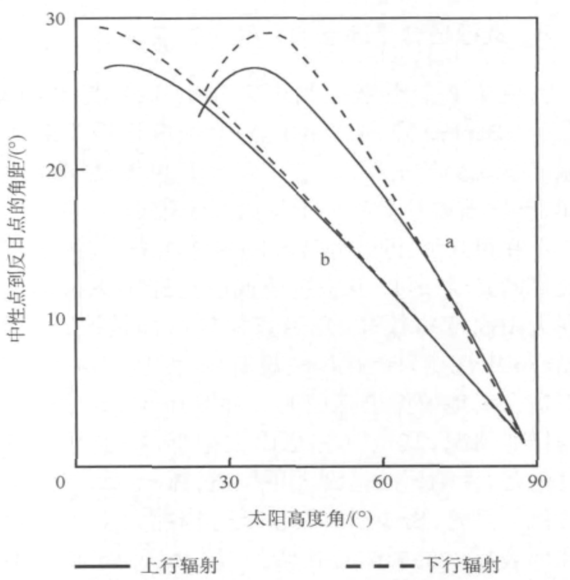

图5 太阳到中性点的角距与太阳高度角的关系曲线

高度角为25°—60°时，两者的位置有了很大的分化；当太阳高度角小于25°时，由于太阳位置较低，上行辐射的 Arago 点与下行辐射的 Brewster 点都无法在天空中出现。对于曲线 b，当太阳高度角约为32°—90°时，上行辐射的中性点(反 Babinet 点)与下行辐射中性点(Babinet 点)的位置完全一致，只有当太阳高度较小(约5°—32°)时，两者的位置才出现差异。

以上情况说明了在大气光学厚度较小、太阳高度角较大时，同一区域天基和地基观测的中性点的位置是一致的。一般情况下，在利用光学卫星对地进行资源探测时，卫星过境时的太阳高度角都比较大，这时可以利用地基观测的中性点的位置去推算天基观测的中性点的位置。

Kattawar 等人(1976)比较了不同大气光学厚度的上行辐射与下行辐射中大气中性点位置。结果表明太阳高度角较大时，Babinet 中性点随着光学厚度的增大而变化很小，但 Brewster 中性点随光学厚度的增大而变化很大。当光学厚度小于5时，上行辐射中反 Babinet 中性点的位置几乎与下行辐射中 Babinet 中性点的位置一致。这也从另外一个角度说明了这种情况下地基观测和天基观测的相同区域的中性点位置的一致性。该文献同时也给出了地表反照率对中性点位置的影响情况。地表反射率的变化对中性点位置的影响并不大，但 Brewster 中性点比 Babinet 中性点对地表反照率的影响更敏感。在上行辐射中反 Babinet 中性点的位置几乎不受地表反照率的影响。

3.2 选取适合于遥感的大气中性点

要从3个空基观测中常见的中性点(Brewster点、反Babinet点和Arago点)中选取适用于对地偏振遥感观测的中性点,首先需要其位置便于遥感观测;其次需要其受外界干扰或影响较小。

在可见光-近红外波段的遥感探测中,为了获取充足的光照条件,卫星过境或航空遥感飞行都选择在太阳高度角较高、光照条件较好的情况下进行,Arago中性点只能在早晚观测到,而且其位置较低,不适合对地偏振遥感观测。对于Brewster中性点有同样的情况,其位置总是比太阳低,特别是在高纬度地区,太阳无法达到天顶位置,Brewster点的位置更低。另外,Brewster点在上行辐射时受大气状况和地表反射的影响也比较大,故Brewster点也不适用于对地偏振遥感。

相对而言,反Babinet中性点则是对地偏振遥感比较理想的选择。由地基观测的Babinet点的性质可知,反Babinet中性点位于太阳的同一侧,其位置始终处于太阳的上方。即反Babinet中性点全白天都可以在天基上观测到,且高度角较大,有利于获取较好的光照条件,便于遥感观测;另外,反Babinet中性点对大气状况及地表反照率不敏感,在大气状况变化时,其位置也较稳定。

3.3 大气中性点位置的计算

鉴于Babinet中性点与反Babinet中性点在太阳高度角较高时位置几乎一致,所以反Babinet的位置可由Babinet点的位置来推算。而Babinet中性点位置的主要影响因素是太阳高度角,所以中性点位置计算的首要问题是确定观测的时间。

太阳高度角的计算公式为:

$$\sin h = \sin\varphi\sin\delta + \cos\varphi\cos\delta \qquad (1)$$

式中,φ是地理纬度,太阳赤纬角δ可以由天文年历查出。根据式(1)可计算出地球上任一点在任一时刻的太阳高度角。

考虑到大气质量,遥感中一般要选择晴好的天气条件进行飞行。对于Babinet中性点,在光学厚度为0.10时,其在主平面上位置与太阳高度有关,如图2所示,其曲线有一定的弯曲,为方便起见,将图中的Babinet中性点曲线分成两个线段进行考虑,即太阳高度角为0—30°和30°—90°时分别拟合为线段。

$$\begin{cases} y = 0.9x + 18 & (0 < x < 30) \\ y = 0.75x + 22.5 & (30 \leqslant x < 90) \end{cases} \qquad (2)$$

式中,x为太阳高度角,y为中性点的高度角。

对于赤道地区有一种特殊情况,当正午太阳高度角为90°时,垂直照射地表,所有的中性点都汇集在太阳点,这时垂直观测地表,偏振传感器会处于中性点区域。

对于非赤道地区,正午时刻的太阳高度角小于90°,可以根据当地时间计算其太阳高度角。由于中性点位于太阳与天顶的主平面上,代入式(2)计算相应的中性点大致位置,得出适合的遥感时间。即使遥感器不能恰好位于天空中性区域的中心,紧邻中性点区域其偏振度较小,也有利于偏振对地观测。

4 地面实验验证

为验证利用中性点进行地-气偏振效应分离方法的可行性,设计了一个地面验证实验。实验是在中性点位置和非中性点位置分别对同一区域进行偏振成像,然后对成像的偏振参数结果进行比较。图6为地面实验验证的观测几何示意图。图中地表与中性点所示的连线上偏振度为零。实验的成像装置是尼康D200单反数码相机,在相机前放置碘偏振片,改变偏振片的透光轴与参考轴的角度,分别获取0°、60°和120° 3个角度下的数据,计算得到偏振参数的图像。

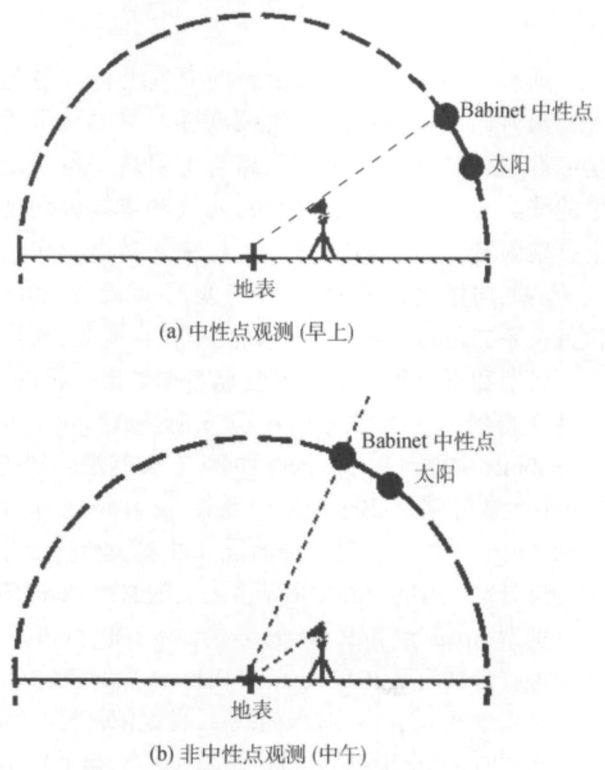

图6 地面实验验证的观测几何示意图

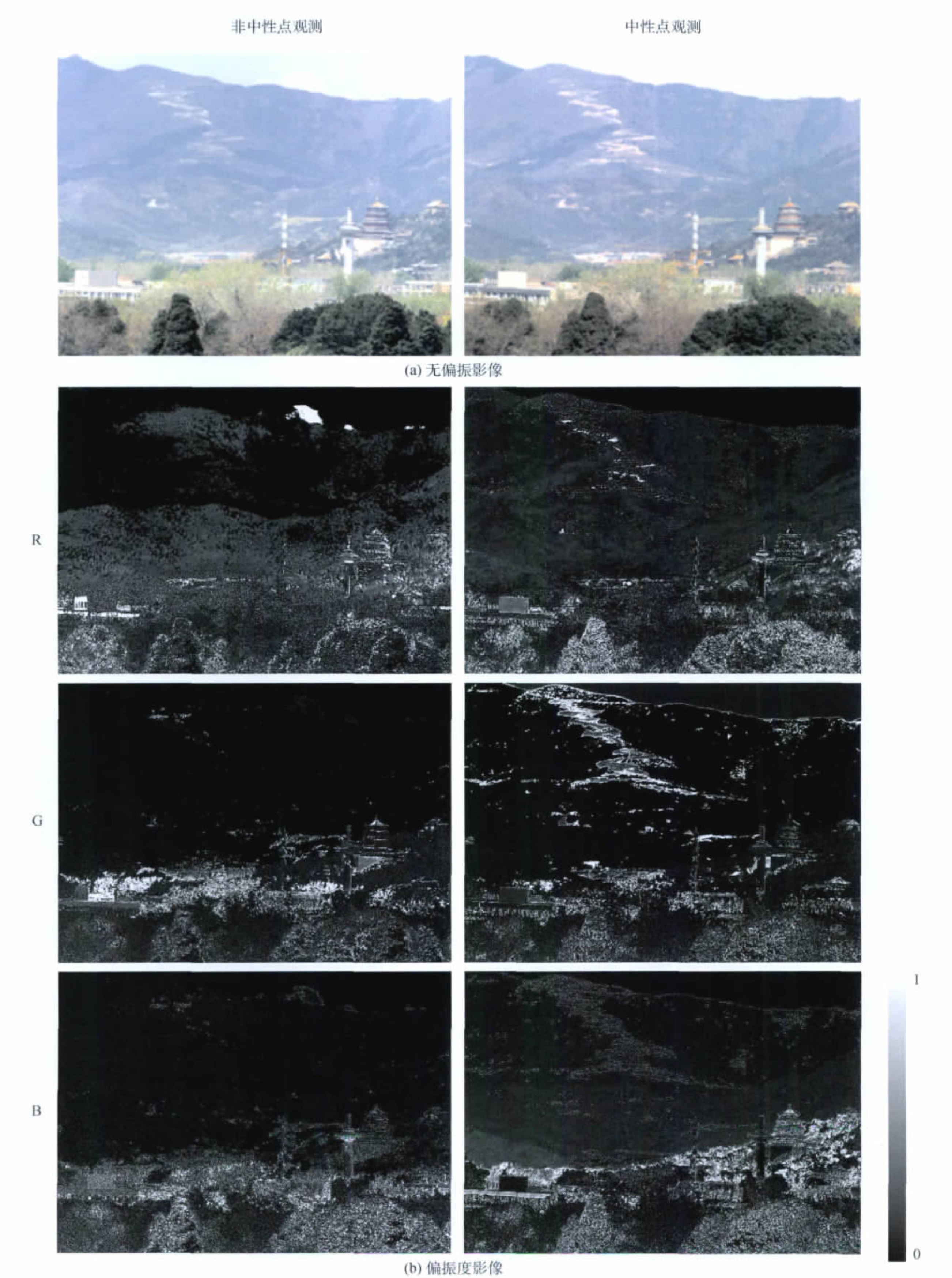

图 7 中性点位置成像与非中性点位置成像的偏振参数对比图

图7为中性点位置成像与非中性点位置成像的偏振参数对比图。观测时间分别为2010年4月29日7:20和11:20,太阳高度角分别约为24.40°和62.95°,根据式(2),中性点的高度角分别为39.96°和69.71°。其时太阳方位角(正南方向定义为零方位)分别为88.55°和21.70°。设定相机在两个时间点拍摄的探测高度角均为40°,相机与太阳的相对方位角分别为0°(后向)和66.85°。天气晴朗无风,观测地点为北京大学遥感楼5楼平台,目标区域为颐和园景区。

图7(a)为没有加偏振片拍摄的图像,大气能见度较高,无论在中性点区域观测还是在非中性点区域观测,图像都比较清晰;图7(b)从上到下分别为红(R)、绿(G)和蓝(B)3个波段的偏振度影像,其影像位数均为8位。偏振度反映了地物偏振程度,取值范围是0—1。图中白色区域表示偏振度大,黑色的区域表示偏振度小。在中性点观测的偏振度影像上,无论近处的颐和园万寿山佛香阁(距拍摄点直线距离约3.1 km),还是远处的西山(距拍摄点直线距离约6—8 km),都清晰可见,特别是山上的裸土(或道路)信息与无偏振图像吻合度较高。并且红、绿和蓝3个波段的影像上所表示的偏振信息也不尽相同。而在非中性点观测的偏振度影像上,近处的地物信息有不错的表现(如佛香阁可见),但远处山的信息却要弱得多,仅能依稀显现山的轮廓。这说明远处山的偏振信息在非中性点观测时无法有效获取。这也说明随着拍摄点到地物的距离增大,大气的偏振效应增大,地物的偏振信息减弱。

将图7(a)无偏振影像、图7(b)的红、绿、蓝3个波段的偏振度影像在Matlab软件中分别进行信息熵计算。从图8(a)中可以看出,非中性点位置成像与中性点位置成像的两组无偏振影像的信息熵几乎相等,但对于红、绿、蓝3个波段的偏振度影像,中性点位置成像的信息熵值均大于非中性点位置成像的信息熵值,这也说明中性点位置的偏振度影像上地物的信息量更大。特别地,如果截取所有图像上半部,即只保留图像中较远地物的影像,再分别进行信息熵计算,其计算结果如图8(b)所示。同样的,两组无偏振影像的信息熵几乎相等,但对于红、绿、蓝3个波段的偏振度影像,中性点位置成像的信息熵值要远大于非中性点位置成像的信息熵值。

从上述的比较结果可见,大气效应对非中性点观测影像的影响比中性点观测影像的影响更强。中性点观测的偏振度影像在反映远距离地物时有更好的表现力,即受大气影响较小。图7中性点观测的偏振度影像上地物的信息量远大于非中性点观测偏振度影像上地物的信息量。这就说明了中性点区域成像可以有效消除大气偏振效应,更大程度上获取地物偏振信息。实验结果表明,利用中性点对偏振遥感进行大气纠正方法具备可行性。

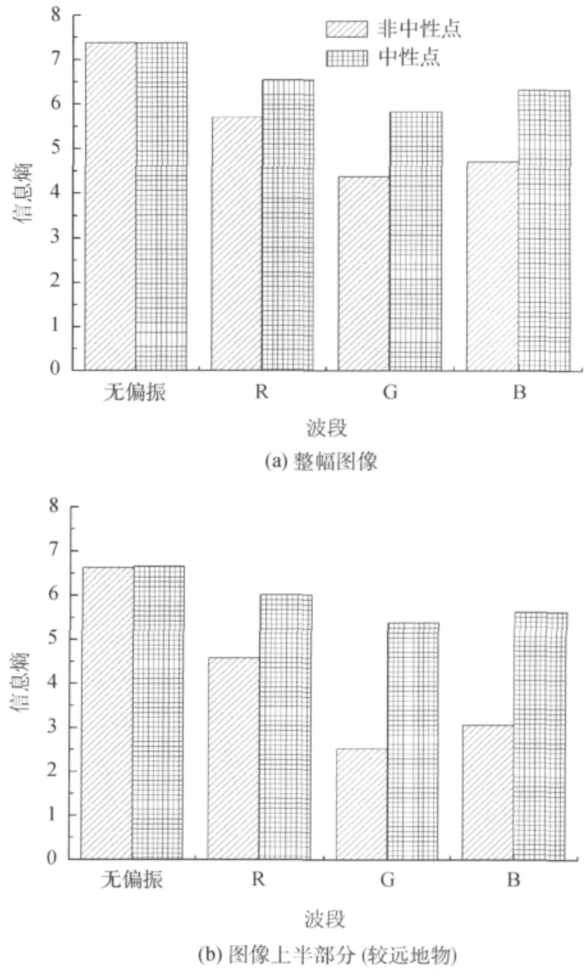

图8 中性点与非中性点位置成像的信息熵对比

5 结论

本文提出了一种利用大气中性点进行偏振遥感地表-大气偏振效应分离的方法,得到以下结论:在天基可以观测到大气中性点;其位置在一定条件下与地基观测的中性点位置一致;且在大气上行辐射观测到的反Babinet中性点更适合于偏振遥感对地观测;利用模型可以计算反Babinet中性点在天空中的位置,以便用于航空遥感中。本文还利用地面偏振成像的方式对该方法进行了实验验证,结果表

明在中性点区域成像可以有效消除图像中大气的偏振效应,突出地物的偏振特性信息。利用中性点进行偏振遥感中大气纠正的方法具有理论与实践的可行性,有较强的现实意义。

参考文献(References)

Bicheron P, Leroy M, Hautecoeur O and Bréon F. 1997. Enhanced discrimination of boreal forest covers with directional reflectances from the airborne polarization and directionality of Earth reflectances (POLDER) instrument. Journal of Geophysical Research, 102 (D24): 29517 - 29529, 29528 [DOI: 10.1029/97JD01330]

Breon F M, Tanre D, Lecomte P and Herman M. 1995. Polarized reflectance of bare soils and vegetation: measurements and models. IEEE Transactions on Geoscience and Remote Sensing, 33(2): 487 - 499 [DOI: 10.1109/36.377949]

Cairns B, Waquet F, Knobelspiesse K, Chowdhary J and Deuzé J L. 2009. Polarimetric remote sensing of aerosols over land surfaces \\ Satellite Aerosol Remote Sensing over Land. New York: Springer: 295 - 325

Chandrasekhar S and Elbert D D. 1954. The illumination and polarization of the sunlit sky on Rayleigh scattering. Transactions of the American Philosophical Society, 44(6): 643 - 728 [DOI: 10.2307/1005777]

Coulson K L. 1959. Characteristics of the radiation emerging from the top of a rayleigh atmosphere—I: Intensity and polarization. Planetary and Space Science, 1(4): 265 - 276 [DOI: 10.1016/0032 - 0633(59) 90031 - 5]

Coulson K L. 1988. Polarization and intensity of light in the atmosphere // Studies in Geophysical Optics and Remote Sensing. Hampton, Va., USA: A. Deepak Publishing: xxv, 596

Fan X H, Goloub P, Deuzé J L, Chen H B, Zhang W X, Tanré D and Li Z Q. 2008. Evaluation of PARASOL aerosol retrieval over North East Asia. Remote Sensing of Environment, 112(3): 697 - 707 [DOI: 10.1016/j.rse.2007.06.010]

Horváth G, Bernath B, Suhai B, Barta A and Wehner R. 2002. First observation of the fourth neutral polarization point in the atmosphere. Journal of the Optical Society of America a-Optics Image Science and Vision, 19(10): 2085 - 2099 [DOI: 10.1364/JOSAA.19.002085]

Horváth G and Varjú D. 2004. Polarized Light in Animal Vision: Polarization Patterns in Nature. New York: Springer Verlag

Kattawar G W, Plass G N and Hitzfelder S J. 1976. Multiple scattered radiation emerging from Rayleigh and continental haze layers. 1: Radiance, polarization, and neutral points. Applied Optics, 15(3): 632 - 647 [DOI: 10.1364/AO.15.000632]

Miyazaki D, Ammar M, Kawakami R and Ikeuchi K. 2009. Estimating sunlight polarization using a fish-eye lens. IPSJ Transactions on Computer Vision and Applications, 1: 288 - 300

Muheim R, Phillips J B and Åkesson S. 2006. Polarized light cues underlie compass calibration in migratory songbirds. Science, 313 (5788): 837 - 839. [DOI: 10.1126/science.1129709]

Nadal F and Bréon F M. 1999. Parameterization of surface polarized reflectance derived fromPOLDER spaceborne measurements. IEEE Transactions on Geoscience and Remote Sensing, 37(3): 1709 - 1718 [DOI: 10.1109/36.763292]

盛裴轩,毛节泰,李建国. 2003. 大气物理学. 北京: 北京大学出版社

Wu T X and Zhao Y S. 2005. The bidirectional polarized reflectance model of soil. IEEE Transactions on Geoscience and Remote Sensing, 43(12): 2854 - 2859 [DOI: 10.1109/TGRS.2005.857905]

Neutral point consideration for atmospheric correction in polarization remote sensing

WU Taixia, ZHANG Lifu, CEN Yi, HUANG Changping, ZHAO Hengqian, SUN Xuejian

Institute of Remote Sensing and Digital Earth, Chinese Academy of Sciences, Beijing 100101, *China*

Abstract: Polarized reflectance of land surface is essential to remote sensing, despite the fact that the reflectance information received by polarimeter is always overwhelmed by atmospheric polarization effect, which is stronger than that of the land objects. Subtracting the atmospheric effect, therefore, is a bottleneck problem in the polarization remote sensing over land surface. Atmospheric neutral point, which refers to a position where the skylight is unpolarized, is introduced in this paper as a tool for separating the polarization effect between objects and atmosphere. The ground experimental results show that when observing the land surface from neutral point, the polarization effect of the atmosphere is reduced to zero and the polarization information of land surface is maximized. The results indicated the feasibility of using atmosphere neutral points for atmospheric correction over land surface.

Key words: polarization remote sensing, neutral point, atmospheric correction

CLC number: TP721.1 **Document code:** A

Citation format: Wu T X, Zhang L F, Cen Y, Huang C P, Zhao H Q and Sun X J. 2013. Neutral point consideration for atmospheric correction in polarization remote sensing. Journal of Remote Sensing, 17(2): 235 – 247

1 INTRODUCTION

Scattered atmospheric particles exhibit strong polarization p henomena. The polarization effect of the atmosphere is the main signal of the polarization remote sensing. For this reason, the present spaceborne polarization remote sensing data are mainly used for a tmospheric research, such as to study the atmosphere physical properties and optical properties (Fan,et al., 2008; Cairns, et al., 2009). Land objects also have strong reflected polarization phenomenon and this it can be valuable information for remote sensing(Breon, et al., 1995; Wu & Zhao, 2005). The land objects detection was one of the tasks of the spaceborne polarimeter-Polarization and Directionality of the earth′s Reflectance (POLDER). However, studies found that the polarization effect of the atmosphere is much stronger than that of land objects in the images. Land objects polarization information r eceived by the polarimeter is always submerged in the atmospheric polarization effect (Bicheron, et al., 1997; Nadal & Bréon, 1999). As a result, a major concern for the use of polarized light for the study of land surfaces is the capability to discriminate between polarization generated in the atmosphere and that generated by the surface.

The neutral point is the point (or area) where the skylight is u npolarized. In the clear sky there are three normally occurring n eutral points, the Arago, Babinet, and Brewster neutral points, in the principal plane (Miyazaki, et al., 2009). In this paper we attempt to set space-borne polarimeter detects the earth at the direction of the neutral point. Because the polarization effect of atmosphere is zero at this direction and then the polarization information of the land surface objects can be maximized. This study would promote the p olarization remote sensing for land objects detection and expand the polarization remote sensing research to a wider research area.

2 ATMOSPHERE POLARIZATION DISTRIBUTION AND NEUTRAL POINT

The solar radiation have no polarization at the outer space, it will be polarized after the atmosphere particles scattering. If most of the atmosphere scattering is single scattering, the polarization of the sky will show a regular polarization distribution, it also known as the polarization pattern of sky.

Under the clear sky weather conditions, in the vertical plane of sun, it will appear the Arago, Babinet, and Brewster neutral points in the sky. As shown in Fig. 1. The Arago normally located 20°—30° above the anti-solar point. The Babinet Point directly above the sun 15°—20°. The Brewster Point directly below the sun varies 15°—20°. Both the Babinet Point and Brewster Point are at the same d irection of sun and their positions changed along with the solar a ltitude. The higher the sun elevation angles the closer between the Babinet Point and the Brewster Point. When the sun is at the zenith, the two points merged as one point (Sheng, et al., 2003; Muheim, et al., 2006). Because the neutral points at two side of sun and anti-solar are symmetry. There should be another neutral point under anti-solar in theory, as the anti-Babinet neutral point. In 2002, the fourth neutral point actually has been detected using the sounding balloon(Horvath, et al., 2002).

For the single scattering, the polarization of the skylight is positive generally. However, for the multiple scattering, the atmospheric

Received: 2012-05-15; **Accepted:** 2012-08-15

Foundation: National Natural Science Foundation of China (No. 41101328, 61178065); The Knowledge Innovation Program of the Chinese Academy of Science

First author biography: WU Taixia (1979—), male, assistant professor, his research interest is the polarization hyperspectral remote sensing. E-mail: wutx@irsa.ac.cn

Corresponding author biography: ZHANG Lifu (1967—), male, professor, his research interest is the hyperspectral remote sensing. E-mail: zhanglf@irsa.ac.cn

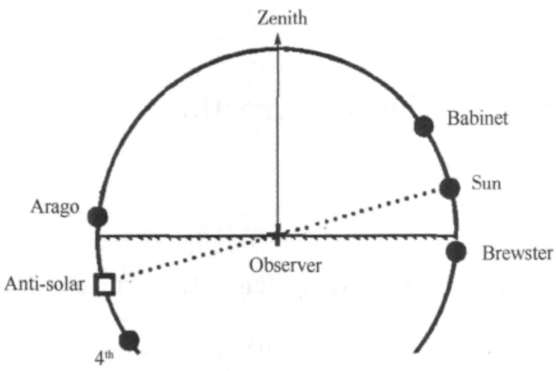

Fig. 1 Normal positions of neutral points in the sky

particles can cause negative polarization. The degree of polarization of sky will be zero where the Positive and negative polarization meet at the intersection area. In this way the atmospheric neutral point produced (Coulson, 1988; Horváth & Varjú, 2004). The Neutral point always at the main plane of the sun and zenith. The stronger the multiple scattering, there will be more negative polarization, and the neutral point position will be farther away from the theory position.

The positions of neutral points are close to the sun elevations. Chandrasekhar calculated positions of the three neutral points for v arious angles of incidence in the main plane (Chandrasekhar & E lbert, 1954). Fig. 2 shows the case for atmospheric optical thickness of 0.10.

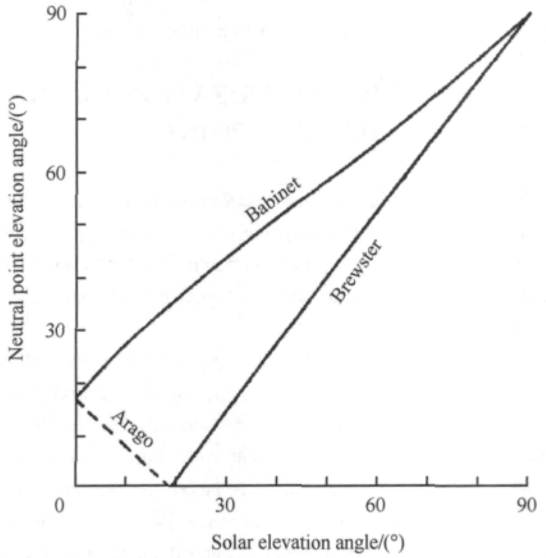

Fig. 2 The position relationship of neutral point and sun

Babinet point is visible throughout the day from before sunrise until after sunset. The Brewster neutral point began visible when solar elevation angle exceeding 20°. The position of the Brewster point and sun are almost linear. As for Arago point, it will appear when solar elevation angle less than 20°, that is the Arago point can only be observed in the morning or evening. The situation of other atmospheric optical thicknesses (0.15 or 0.20) is almost the same.

3 ATMOSPHERE CORRECTION METHOED BASED ON NEUTRAL POINT

The method of using atmospheric neutral point for polarization remote sensing is to set the remote sensing sensor at the direction of the neutral point. At this moment, the atmospheric polarization effect between sensor and land objects can be zero or minimized. The p olarization information of land objects received by sensor can be maximized. Fig. 3 is the sketch map of using neutral points for polarization remote sensing atmosphere correction. The dash circle is v irtual the outer of the Earth atmosphere. This circle also is the sun trail of the very day. The sun position in the figure is a virtual position too, which only denote the direction of the sun in the figure. From space to land surface, the neutral point can be seen at each height in the line goes through the neutral point and land object in theory. So the neutral point can be observed whether by airborne or space borne sensors.

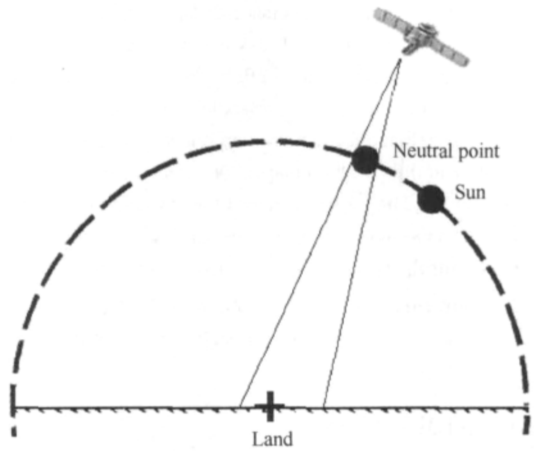

Fig. 3 Sketch map of using neutral points for polarization remote sensing atmosphere correction

In the real atmosphere, because of multiple scattering, the neutral point probably not a point but a small region where all the degree of polarization close to zero. In addition, this neutral point (region) in the sky also not a fixed position, but a conical region which starting point is the sensor as shown in Fig. 3. The atmosphere degree of polarization at any height of this conical region is zero.

3.1 Neutral point characteristics observed from space

The positions of neutral points that we discussed above are based on ground observations, however, remote sensing is a process observed from sky to land. Can the remote sensing sensor detect the neutral point from sky? It is the basic problem of using the neutral point for land surface polarization remote sensing.

Horváth (2002) took the neutral point photos on the ground and at a 3500 m sounding balloon separately. As the dark areas shown in Fig. 4. The local solar elevation angle shooting were similar to 0 when photos. The black spot at the top of the image is the sun. The camera band was red. The Fig. 4 (a) was the ground photo while the Fig. 4 (b) was the balloon photo. The right picture of Fig. 4 (b) indicates the neutral point can be observed from space.

Coulson (1959) calculated the neutral point position of the a tmosphere upward radiation and the downward radiation. Fig. 5 shows the curve of angular distance between the sun and the neutral points as a function of sun elevation. The atmosphere optical thickness is 1.0. The solid curves are the upward radiation and the dash curves are the downward radiation. The upward radiation is caused by the atmospheric particles back scattering. The neutral point's p ositions are different in the upward radiation and the downward r adiation. So the neutral points have different names in the upward ra-

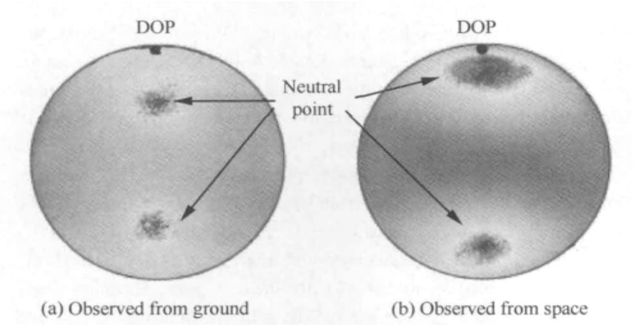

Fig. 4 The neutral point observed from ground and space

diation and the downward radiation. The neutral points observed from ground are Arago point, Babinet point and Brewster point. And the corresponding neutral points observed from the space are Brewster point, anti-Babinet point and Arago point.

In Fig. 5, the solid and dash lines of curve a denote the neutral point below the anti-solar and solar separately, they are Arago point and Brewster point. The solid and dash lines of curve b denote anti-Babinet point and Babinet point separately.

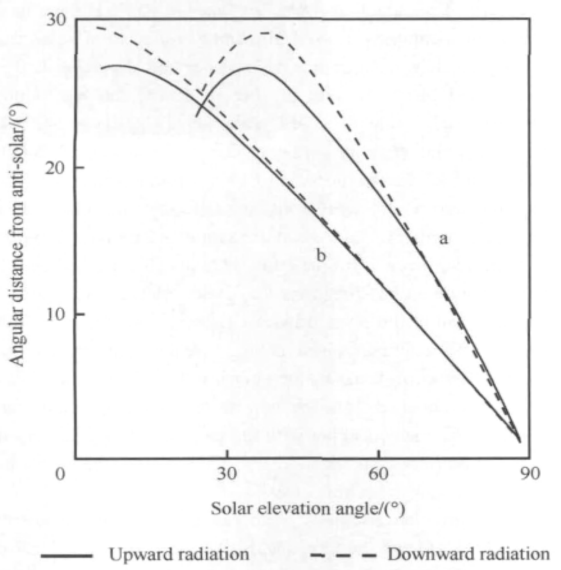

Fig. 5 Angular distance between the sun and the neutral points

It can be seen from Fig. 5, as for curve a, the neutral point positions in the upward and downward radiation are completely the same when the solar elevation angle is about 60°—90°. Their positions began different greatly when the solar elevation angle from 25° to 60°. Both the neutral points in the upward (Arago point) and downward (Brewster point) radiation cannot appear in the sky when the solar elevation angle less than 25°. As for curve b, the two neutral points′ positions in the upward (anti-Babinet point) and downward radiation (Babinet point) are entirely consistent when the solar elevation angle is about 32°—90°. Only when the solar elevation angle is small (about 5°—32°), the positions began different slightly.

The above discussion showed that the neutral point positions of the same area observed from space and ground are consistent when the atmosphere optical thickness is small and the solar elevation angle is big. Normally, satellite transit time or aerial remote sensing flight time always chose a high solar elevation, in order to obtain sufficient light conditions. At this time, the space-based neutral point position can be calculated by the ground-based observation position.

Kattawar(1976) compared the neutral point positions of different atmosphere optical thicknesses in the upward and downward r adiation. The result shows that when the atmosphere optical thickness increased, the Babinet Point position change slightly while the Brewster Point changed greatly. The position between anti-Babinet point in the upward radiation and Babinet point in the downward radiation are almost the same when the atmosphere optical thickness less than 5. This also indicates that the Babinet point positions of the ground-based and space-based observations are coincident of the same area. This paper was also given the impact of the surface albedo on the neutral point position. The change of s urface albedo has small effect to the neutral point position. But the Brewster point is more sensitive than the Babinet point on the surface albedo impact. The anti-Babinet point in the upward radiation is independent of surface albedo.

3.2 Proper neutral point selected for remote sensing

There are three common neutral points in the sky. We need s elect the most applicable one for the polarization remote sensing. The first satisfy condition is its position in the sky convenience for remote sensing observation. The second condition is its position should more stable.

In the visible-near infrared remote sensing, satellite transit time or aerial remote sensing flight time always chosen a higher solar e levation, in order to obtain sufficient light conditions. The Arago neutral point can only observed in the morning or toward evening. And its position in the sky is low when it appears. Its position is a lways lower than sun. Especially in high latitude area, the sun cannot reach the zenith position. The Arago point is not suitable for p olarization remote sensing. The Brewster neutral point has the same situation. The Brewster point position is bound to be even lower. In addition, the Brewster point effected by the atmosphere condition and land surface reflection greatly. So the Brewster neutral point is also not suitable for polarization remote sensing.

In contrast, the anti-Babinet neutral point is an ideal choice for polarization remote sensing. From the earth observed characters of Babinet neutral point, the anti-Babinet point is in the same side of the sun; its position is always higher than the sun. That is the anti-Babinet point can be observed all the day. The higher elevating angle is benefit in remote sensing to obtain better light conditions. Moreover, the anti-Babinet point is not sensitive to the atmosphere condition. Its position is more stable in the sky when the atmosphere c ondition changes.

3.3 The position of neutral point calculated

The position of the anti-Babinet neutral point can be calculated from the position of the Babinet neutral point, since the two points almost have the same position.

The main factor of the anti-Babinet point position is the solar elevation. So when using anti-Babinet point for land surface polarization observation, the first thing is to determine the observation time.

The solar elevation angle is constantly changing at the same place a day. The sun elevation angle of a place can be calculated by the solar elevation angle formula.

$$\sin h = \sin\varphi\sin\delta + \cos\varphi\cos\delta \quad (1)$$

where h is the solar elevation angle, φ stand for the local geographical latitude, δ is the solar declination angle and τ is solar hour angle.

Generally, it is selected good weather conditions for aerial remote sensing flight. For the anti-Babinet neutral point, its position in the main plane is the function of the sun elevation when the optical thickness is 0.10. As shown in Fig. 2, the function curve has a certain bent. For convenience, the curve was separated into two parts. Both curves fit as segments.

$$\begin{cases} y = 0.9x + 18 & (0 < x < 30) \\ y = 0.75x + 22.5 & (30 \leqslant x < 90) \end{cases} \quad (2)$$

where x is the solar elevation angle, y is the Babinet neutral point e levation angle.

For the equatorial region, the solar elevation angle of 90° at noon, the sun illuminates the land surface vertically. All the neutral points are gathered into the sun position. The polarization remote sensing sensor should in the neutral point region when observing land surface vertically. This is a special case.

For non-equatorial regions, the sun elevation angle cannot reach 90° at noon. The local noon solar elevation angle can be calculated by Eq. (1). Because neutral point and sun both are at the main plane, the corresponding neutral point position can be calculated from E q. (2). And then get the remote sensing time. One thing need to note, e ven the sensor in the sky cannot exactly at the center of the neutral point, the region around the neutral point also a small polarization area; it is also conducive to polarization observation.

4 EXPERIMENTAL VERIFICATION

In order to verify the method of using the neutral point for p olarization remote sensing, we designed a ground verification e xperiment. Polarization images were taken and compared from n eutral point direction and non-neutral point direction for the same area. Fig. 6 are the observation geometry sketch map. The degree of polarization of atmosphere is zero on the line goes through the neutral point and camera. The imaging device was Nikon D200 digital camera with iodine polarizer. 0°, 60° and 120° three anglesp olarization images were obtained by changing the angle between polarizer transmission axis and reference axis three times. And then the images of polarization parameters such as degree of polarization, polarization angle were calculated.

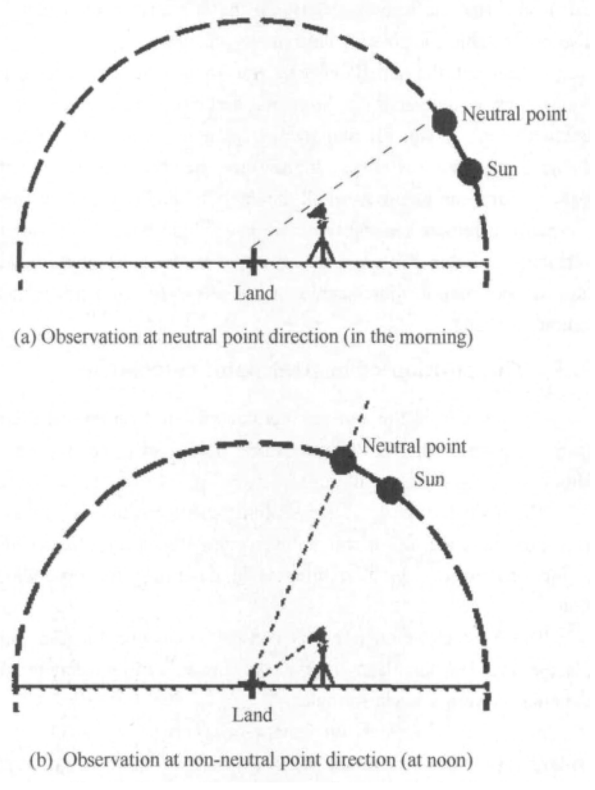

Fig. 6 Observation geometry sketch map of ground verification experiment

Fig. 7 are the polarization parameters comparison images between neutral point imaging and non-neutral point imaging. The observation time was 7:20 am and 11:20 am separately, April 29th, 2010. At that time, the solar elevation angle was 24.40° and 62.95° separately. According to Eq. (2), the neutral point elevation angle was 39.96° and 69.71° separately. The solar azimuth was 88.55° and 21.70° (the south is defined as the zero azimuth) separately. Both the camera detection elevation angle was set as 40°. The relative azimuth angle of the camera and the sun were 0° (backward) and 6 6.85°. The weather was clear and calm. Observation spot was 5th floor platform, Remote sensing Building, Peking University. The target area is Summer Palace scenic region.

Fig. 7 (a) is the images without polarizer. The atmosphere visibility is high. Both the images are clear whether observation at the neutral point direction or non-neutral point direction. Fig. 7 (b) is the linear degree of polarization (DOLP) images of R, G, B three bands. Degree of polarization is a physical quantity reflects the polarization size of objects. It is a dimensionless number and the value is 0—1. The white and black areas in the Figure denote the big value of DOLP and small value of DOLP separately. On the image taken from neutral point direction, whether the closer tower of Buddhist Incense (about 3.1 km from camera) or the forane mountain (about 8 km from camera) are clearly visible, especially the bare soil and road in the mountains. And the polarization information is not the same in the red, green and blue band. However, on the image taken from non-neutral point direction, the closer objects are good displayed, such as the tower of Buddhist Incense. But the polarization information of the forane objects is much weaker, only the mountain outline can be shown. It means the polarization information of forane objects cannot obtained from the non-neutral point direction image. This phenomenon shows along with the increase of the focusing distance, the atmospheric polarization effects increased, the polarization information of targets becomes weak.

The information entropies were calculated of the unpolarized images in Fig. 7 (a) and the three bands of DOLP images in Fig. 7 (b), as shown in Fig. 8 (a). The abscissa is different images and the ordinate is the value of information entropy. The twill denotes entropy value of the non-neutral point imaging and the plaid denotes entropy value of the neutral point imaging. It can be seen from the Fig. 8 (a), the information entropies of the two unpolarized images are almost equal regardless of the neutral point imaging or non-neutral point imaging. However, for the DOLP images of red, green and blue bands, the information entropy values of the neutral point imaging are all greater than the non-neutral point imaging's. This also shows land objects on the neutral point DOLP imaging are informative. In particular, we cut out the upper half of all the images, keep only the distant objects on the images. And then the information entropies were calculated separately. The results showed in Fig. 8 (b). Similarly, the information entropies of the two unpolarized images are almost the same. But for the DOLP images of red, green and blue bands, the information entropy values of the neutral point imaging are all much greater than that of the non-neutral point imaging.

It is thus clear that the atmospheric polarization effect on the non-neutral point direction image is stronger than the neutral point direction image. The degree of polarization image from neutral point

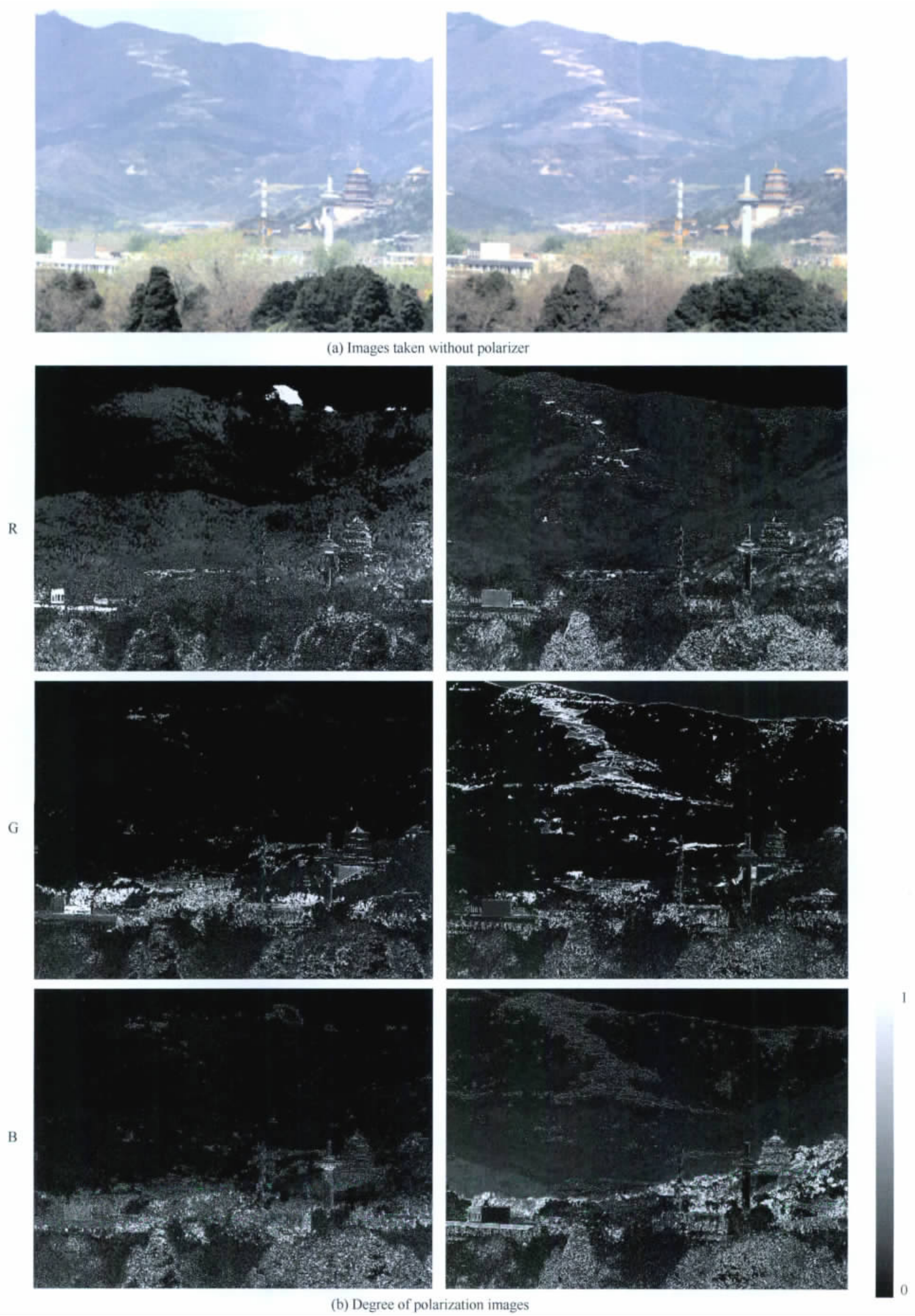

Fig. 7 The polarization collation images between neutral point imaging and non-neutral point imaging

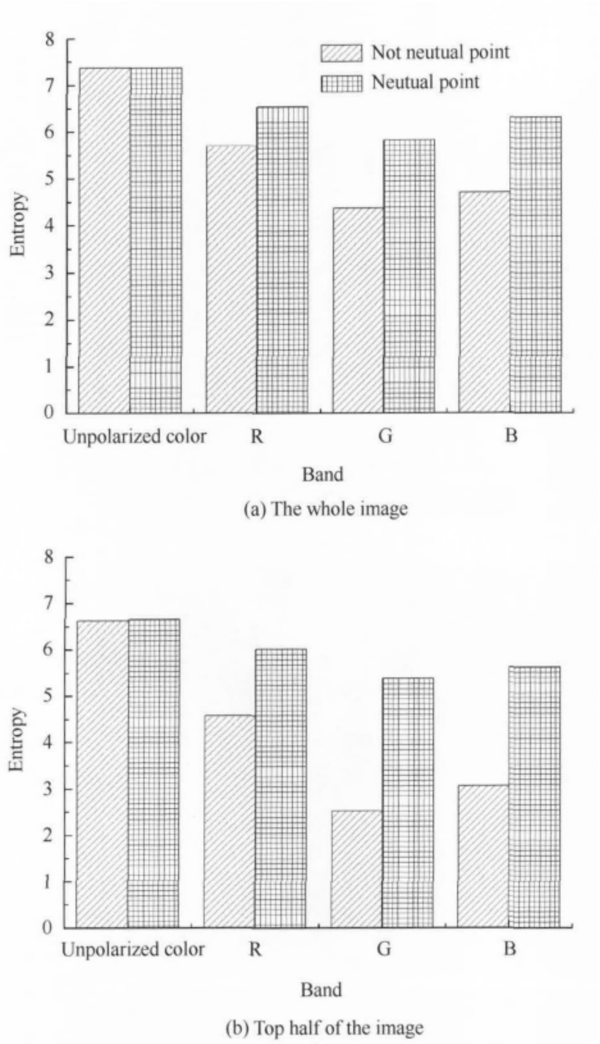

Fig. 8 The information entropy comparison between neutral point and non-neutral point imaging

direction has good expressive force for remote objects. The objects polarization information on it is far greater than on non-neutral point direction image's. It means the neutral point imaging can eliminate the atmospheric polarization effect and enhance the objects polarization information. This experiment demonstrated the feasibility of using neutral point for polarization remote sensing atmospheric correction.

5 CONCLUSION

In this paper, we have presented an approach for using atmospheric neutral points for atmosphere correction in polarization remote sensing. By comparing the position of the neutral points between the downward radiation and the upward radiation, the neutral point can be observed not only from ground but also from the space. The anti-Babinet neutral point observed form space is a good choice for the polarization land surface remote sensing because the position of the Babinet Point is relatively stable. The anti-Babinet neutral point p osition in the sky can be calculated by models for aerial remote sensing. A ground experiment was performed to verify the method. The experiment result shows the images taken from the neutral point direction can eliminate the atmospheric polarization effect effectively and enhance the objects polarization information. This study has demonstrated the feasibility in theory and practice of using atmosphere n eutral point for atmospheric correction.

REFERENCES

Bicheron P, Leroy M, Hautecoeur O and Bréon F. 1997. Enhanced discrimination of boreal forest covers with directional reflectances from the airborne polarization and directionality of Earth reflectances (POLDER) instrument. Journal of Geophysical Research, 102 (D24): 29517 - 29529, 29528 [DOI: 10.1029/97JD01330]

Breon F M, Tanre D, Lecomte P and Herman M. 1995. Polarized reflectance of bare soils and vegetation: measurements and models. IEEE Transactions on Geoscience and Remote Sensing, 33(2): 487 - 499 [DOI: 10.1109/36.377949]

Cairns B, Waquet F, Knobelspiesse K, Chowdhary J and Deuzé J L. 2009. Polarimetric remote sensing of aerosols over land surfaces \\ Satellite Aerosol Remote Sensing over Land. New York: Springer: 295 - 325

Chandrasekhar S and Elbert D D. 1954. The illumination and polarization of the sunlit sky on Rayleigh scattering. Transactions of the American Philosophical Society, 44(6): 643 - 728 [DOI: 10.2307/1005777]

Coulson K L. 1959. Characteristics of the radiation emerging from the top of a rayleigh atmosphere—I: Intensity and polarization. Planetary and Space Science, 1(4): 265 - 276 [DOI: 10.1016/0032-0633(59) 90031 - 5]

Coulson K L. 1988. Polarization and intensity of light in the atmosphere // Studies in Geophysical Optics and Remote Sensing. Hampton, Va., USA: A. Deepak Publishing: xxv, 596

Fan X H, Goloub P, Deuzé J L, Chen H B, Zhang W X, Tanré D and Li Z Q. 2008. Evaluation of PARASOL aerosol retrieval over North East Asia. Remote Sensing of Environment, 112(3): 697 - 707 [DOI: 10.1016/j.rse.2007.06.010]

Horváth G, Bernath B, Suhai B, Barta A and Wehner R. 2002. First o bservation of the fourth neutral polarization point in the atmosphere. Journal of the Optical Society of America a-Optics I mage Science and Vision, 19(10): 2085 - 2099 [DOI: 10.1364/JOSAA.19.002085]

Horváth G and Varjú D. 2004. Polarized Light in Animal Vision: Polarization Patterns in Nature. New York: Springer Verlag

Kattawar G W, Plass G N and Hitzfelder S J. 1976. Multiple scattered r adiation emerging from Rayleigh and continental haze layers. 1: Radiance, polarization, and neutral points. Applied Optics, 15(3): 632 - 647 [DOI: 10.1364/AO.15.000632]

Miyazaki D, Ammar M, Kawakami R and Ikeuchi K. 2009. Estimating sunlight polarization using a fish-eye lens. IPSJ Transactions on Computer Vision and Applications, 1: 288 - 300

Muheim R, Phillips J B and Åkesson S. 2006. Polarized light cues underlie compass calibration in migratory songbirds. Science, 313 (5788): 837 - 839. [DOI: 10.1126/science.1129709]

Nadal F and Bréon F M. 1999. Parameterization of surface polarized r eflectance derived fromPOLDER spaceborne measurements. IEEE Transactions on Geoscience and Remote Sensing, 37(3): 1709 - 1718 [DOI: 10.1109/36.763292]

Sheng P X, Mao J T and Li J G. 2003. Atmospheric Physics. Beijing: Peking University Press

Wu T X and Zhao Y S. 2005. The bidirectional polarized reflectance model of soil. IEEE Transactions on Geoscience and Remote Sensing, 43(12): 2854 - 2859 [DOI: 10.1109/TGRS.2005.857905]